IDENTIFICATION OF COAXIAL-ROTORS DYNAMIC WAKE INFLOW FOR FLIGHT DYNAMICS AND AEROELASTIC APPLICATIONS

Felice Cardito, Riccardo Gori, Giovanni Bernardini
Jacopo Serafini, Massimo Gennaretti

Department of Engineering, University Roma Tre, Rome, Italy

Abstract

This paper presents the development of a linear, finite-state, dynamic perturbation model for wake inflow of coaxial rotors in arbitrary steady flight, based on high-accuracy radial and azimuthal representations. It might conveniently applied in combination with blade element formulations for rotor aeroelastic modelling, where three-dimensional, unsteady multiharmonic and localized aerodynamic effects may play a crucial role. The proposed model is extracted from responses provided by an arbitrary high-fidelity CFD solver to perturbations of rotor degrees of freedom and controls. The transfer functions of the multiharmonic responses are then approximated through a rational-matrix approach, which returns a constant coefficient differential operator relating the inflow multiharmonic coefficients to the inputs. The accuracy of the model is tested both for hovering and forward flight by comparison with the wake inflow directly evaluated by the high-fidelity CFD tool for arbitrary inputs.

1. INTRODUCTION

Due to the improved performance they may provide, coaxial rotors are expected to become a common solution for next-generation rotorcraft.

Indeed, as the forward flight speed increases, the difference of dynamic pressure between the advancing and retreating sides of a single rotor becomes greater, making necessary higher values of the cyclic pitch to maintain the aircraft trimmed. In order to avoid blade stall on the retreating side of the rotor disk, the amount of collective pitch has to be correspondingly reduced, thus negatively affecting the rotor thrust capability.[1]

In coaxial, contra-rotating rotors the advancing blades of each rotor may operate at higher pitch angles to produce more lift without compromising roll trim. At the same time, the retreating blade may be kept far from stall, with two major consequences: i) rotor RPM may be reduced, increasing the speed at which transonic effects arise at the tip of advancing blades, and ii) the overall vibratory loads transmitted to the fuselage are strongly reduced, thus allowing the employment of stiffer blades that improve helicopter manoeuvrability.[2] In addition, the maximum lift-to-drag ratio is improved: the coaxial rotors have proven to be intrinsically more efficient in hover, forward flight than single rotors of the same solidity and blade geometry. Furthermore, coaxial rotors provide torque cancellation, thereby eliminating the need for a tail rotor and its associated shafting and gearboxes.

While coaxial rotors have been investigated since the begin of aeronautics, for decades, the increased complexity of rotor hub suggested the manufacturers to use simpler main-tail rotor configurations. Nowadays, the difficulties in overcoming the limits of single rotor helicopters resulted in a growing interest for coaxial rotor configurations as demonstrated by the Sikorsky X2 and the Kamov Ka-92 projects, among the others.

This fact motivates the development of dedicated computational tools suited for their analysis. Dynamic wake inflow modeling is one of the main issues in efficient and reliable rotorcraft simulation tools concerning aeroelasticity, flight mechanics, and handling quality assessment, as well as for flight control laws definition.[3–5] The most widely used dynamic inflow models for single rotors (see for instance, Refs. [6,7]) cannot be extended to coaxial rotors with satisfactory accuracy, due to the importance of the aerodynamic interaction effects occurring.

This paper presents the development of a linear, finite-state, dynamic perturbation model for wake inflow of coaxial rotors in arbitrary steady flight, based on high-accuracy radial and azimuthal representations. It is extracted through a numerical process starting with the evaluation of wake inflow corresponding to perturba-

tions of rotor degrees of freedom and controls by a high-fidelity CFD solver. Next the transfer functions of the multiharmonic responses are identified, and then approximated through a rational-matrix approach. This returns constant coefficient differential operators relating the inflow multiharmonic coefficients to the input perturbations (see later for details). Here the wake inflow responses are evaluated through simulations provided by a Boundary Element Method (BEM) tool for potential-flow solutions, suited for rotors in arbitrary motion.[8] It is capable of taking into account free-wake and aerodynamic interference effects in multi-body configurations, as well as the effects due to severe blade-vortex interactions.

The wake inflow modelling presented here may be considered as a direct extension to coaxial rotors of the formulation introduced in Ref. [9] for isolated rotors which, in turn, extended the LTI, finite-state wake inflow modelling approach presented in Ref. [10] to include the multi-harmonic effects related to the intrinsic time-periodic nature of advancing, rotor aerodynamics, as well as the complex radial distributions induced by the wake-blade interactions.

Considering a coaxial rotor in hovering and advancing flight conditions, the numerical investigation presents the identified transfer functions and the assessment of the accuracy of the proposed dynamic inflow model by comparison with wake inflow directly calculated by the time-marching BEM solver. Particular attention is focused on the examination of the capability of capturing radial distributions and multi-harmonic components arising in forward flight.

2. WAKE INFLOW MODELLING

The multi-harmonic wake inflow perturbation model presented here is suited for coaxial rotors aeroelastic applications, and is an extension of those proposed by the authors in Refs.[9–11]

The main steps of the process of wake inflow model extraction from arbitrary high-fidelity aerodynamic solver are: definition of a suited approximation form of the inflow distributions; LTI representation of the model parameters identified from responses of the aerodynamic solver; finite-state approximation of the parameters dynamics, and hence of the inflow model.

The model inputs are the rotor degrees of freedom and controls (in this case including upper and lower rotor blade collective and cyclic pitches). Its accuracy depends on that of the CFD solver used for the evaluation of the aerodynamic responses. Since derived from a high-fidelity aerodynamic solver, it might be applicable to arbitrary multi-body rotor configurations and flight conditions.

2.1. Inflow Representation

In order to represent the complex wake inflow field over a rotor blade with a level of accuracy suitable for (high-frequency) aeroelastic applications, it is expressed in a non-rotating frame in terms of spanwise-varying multiblade variables.

Indeed, introducing over the rotor disc the hub-fixed polar coordinate system, (r, ψ), for (both upper and lower) three-bladed rotors (typically considered in coaxial rotor configurations), the perturbation wake inflow, v, is represented through the following extension of the form applied in the Pitt-Peters model[6, 12]

$$(1)\quad v(r,\psi_i,t) = v_0(r,t) + v_c(r,t)\cos\psi_i + v_s(r,t)\sin(\psi_i)$$

where ψ_i denotes the azimuth position of the i-th blade, whereas v_0, v_c and v_s are, respectively, the instantaneous multiblade collective and cyclic inflow coefficients at a given radial position, r (see also Ref. [9] for higher number of rotor blades).

For v_i denoting the wake inflow perturbation evaluated by the high-fidelity aerodynamic tool on the i-th rotor blade, applying the separation of variables technique, and choosing suitable sets of linearly independent radial basis functions, $\phi_j^\alpha(r)$, the multiblade wake inflow coefficients are expressed in the following form

$$(2)\quad \begin{aligned} v_0(r,t) &= \frac{1}{N_b}\sum_{i=1}^{N_b} v_i(r,t) = \sum_{j=1}^{N_r^0} \lambda_j^0(t)\ \phi_j^0(r) \\ v_c(r,t) &= \frac{2}{N_b}\sum_{i=1}^{N_b} v_i(r,t)\cos\psi_i = \sum_{j=1}^{N_r^c} \lambda_j^c(t)\ \phi_j^c(r) \\ v_s(r,t) &= \frac{2}{N_b}\sum_{i=1}^{N_b} v_i(r,t)\sin\psi_i = \sum_{j=1}^{N_r^s} \lambda_j^s(t)\ \phi_j^s(r) \end{aligned}$$

where N_b denotes the number of rotor blades, N_r^α is the number of functions used to define the α-coefficient radial distribution, with λ_j^α representing the corresponding component onto the basis function ϕ_j^α. It is worth noting that, for $N_r^0 = N_r^c = N_r^s = 1$, $\phi_1^0 = 1$, and $\phi_1^c = \phi_1^s = r$, the proposed inflow distribution coincides with that of the Pitt-Peters model.[6, 12]

2.2. Model Parameters Extraction

The extraction of the dynamic wake inflow model from high-fidelity aerodynamics starts with the identification

of the transfer functions relating the perturbations of the system state variables (namely, rotor rigid and elastic degrees of freedom) with the components of the inflow multiblade coefficients.

To this purpose, following an approach similar to that used in Refs. [9–11], first, a high-fidelity aerodynamic tool is applied to evaluate the blade wake-inflow perturbations, $v_i(r,t)$, corresponding to harmonic small perturbations of the fixed-frame variables, q_k, associated to the state variables of interest.

In this context, it is important to observe that, the time-periodic nature of rotor aerodynamics yields multi-harmonic responses to single-harmonic inputs, with multiplicity related to the number of blades (differently from single rotor configurations, for coaxial rotors this is true also in axi-symmetric hovering operating conditions). For instance, for small-perturbation harmonic cyclic inputs of frequency ω, non-zero harmonic components of the corresponding cyclic outputs appear at the frequencies ω, $mN_b\Omega - \omega$, and $mN_b\Omega + \omega$, for $m = 1, 2, ..., N_m$, with N_m related to the maximum order of periodicity of the aerodynamic operator (see also Ref. [9] for further details).

Therefore, it is convenient to express each inflow component, λ_j^α, in Eq. (2) through the following time-dependent coefficient Fourier series of fundamental frequency $N_b\Omega$

$$\begin{aligned}\lambda_j^\alpha(t) &= \lambda_j^{\alpha,0}(t) \\ &+\sum_{m=1}^{N_m}\left[\lambda_{j,m}^{\alpha,c}(t)\cos(m\,N_b\,\Omega\,t) + \lambda_{j,m}^{\alpha,s}(t)\sin(m\,N_b\,\Omega\,t)\right]\end{aligned} \tag{3}$$

Indeed, for a given harmonic input q_k at frequency ω, the corresponding harmonic components of λ_j^α at the same frequency coincide with those of $\lambda_j^{\alpha,0}$, whereas from its harmonic components at the frequencies $(m\,N_b\Omega - \omega)$ and $(m\,N_b\Omega + \omega)$ it is possible to determine the harmonic components of $\lambda_{j,m}^{\alpha,c}$ and $\lambda_{j,m}^{\alpha,s}$ at frequency ω. The harmonic components at frequency ω of the inflow parameters, $\lambda_j^{\alpha,0}$, $\lambda_{j,m}^{\alpha,c}$ and $\lambda_{j,m}^{\alpha,s}$, suitably combined with the input harmonic component, provide the complex values, at this frequency, of the transfer functions $H_{jk}^{\alpha,0}$, $H_{jk,m}^{\alpha,c}$, $H_{jk,m}^{\alpha,s}$ relating them to the input, q_k.

The proposed identification procedure has to be applied to both upper and lower rotor wake inflow representation.

2.3. Finite-State Approximation

The transfer functions between inputs and the (upper and lower rotor) inflow parameters introduced in Eq. (3) represent LTI dynamics, thus allowing the description of a LTP operator through combination of outputs of LTI sub-operators.

Upper and lower wake inflow dynamics are described in finite-state form by representing the LTI dynamics of the $\lambda_{j,m}^{\alpha,c}$ parameters introduced in Eq. (3) (and collected in the vector $\boldsymbol{\lambda}$) through the following transfer-matrix form

$$\tilde{\boldsymbol{\lambda}} = \mathbf{H}(s)\,\tilde{\mathbf{q}} \tag{4}$$

where s is the Laplace-domain variable, the matrix $\mathbf{H}$ collects all the transfer functions extracted from the aerodynamic responses, whereas $\mathbf{q}$ denotes the vector of the inputs of interest (expressed through fixed-frame/multiblade variables).

Considering the frequency domain of interest of the problem the inflow model is identified for, the process of evaluation of matrix $\mathbf{H}$ is repeated for a discrete number of frequencies within that range, so as to get an adequate sampling of it. Then, the rational-matrix approximation (RMA) of the following form

$$\mathbf{H}\,(s) \approx s\,\mathbf{A}_1 + \mathbf{A}_0 + \mathbf{C}\,[s\,\mathbf{I} - \mathbf{A}]^{-1}\,\mathbf{B} \tag{5}$$

that provides the best fitting of the sampled $\mathbf{H}$-matrix values is determined through a least-square technique.[13] $\mathbf{A}_1, \mathbf{A}_0, \mathbf{B}$ and $\mathbf{C}$ are real, fully populated matrices, whereas $\mathbf{A}$ is a square block-diagonal matrix containing the poles of the approximated transfer functions.

Finally, transforming into time domain the combination of Eqs. (4) and (5) provides the following LTI, finite-state model for the wake inflow parameters

$$\begin{aligned}\boldsymbol{\lambda} &= \mathbf{A}_1\,\dot{\mathbf{q}} + \mathbf{A}_0\,\mathbf{q} + \mathbf{C}\,\mathbf{r} \\ \dot{\mathbf{r}} &= \mathbf{A}\,\mathbf{r} + \mathbf{B}\,\mathbf{q}\end{aligned} \tag{6}$$

where $\mathbf{r}$ is the vector of the additional states representing wake inflow dynamics.

The above LTI differential model relating rotor kinematics to inflow parameters, combined with Eq. (3) provides a LTP operator for the wake inflow components. Applying these components in Eq. (2) and coupling with Eq. (1) yields a space-time accurate LTP prediction model of the wake inflow on upper and lower rotor discs, suitable for aeroelastic (and flight dynamics) applications.

Eliminating the multi-harmonic cyclic terms from Eq. (3), the wake inflow components operator would becomes of LTI type, like that of the wake inflow model

extraction approach introduced in Ref. [11], for low-frequency flight dynamics applications. The inclusion of the multi-harmonic cyclic terms improves the accuracy of the predicted wake inflow (particularly, the higher frequency content).

3. NUMERICAL RESULTS

In this section, the proposed space-time accurate wake inflow model is verified and validated.

Considering a coaxial rotor system composed of two identical three bladed rotors having radius $R = 5.48$ m, blade root chord $c = 0.54$ m, taper ratio equal to 0.5, twist $\theta = -7^\circ$ and counter rotating at angular velocity $\Omega = 32.8$ rad/s, the proposed wake inflow model is assessed for both hovering condition and forward flight at $\mu = 0.2$. Wake inflow transfer functions and their rational approximations are examined, along with the capability of the resulting finite-state model to predict wake inflow radial distribution and time evolution due to arbitrary blade pitch control perturbations.

The rotor wake in the aerodynamic BEM solver is assumed to have a prescribed helicoidal shape that, in forward flight, coincides with the surface swept by the trailing edges, whereas in hovering has a spiral length related to the mean thrust coefficient. In addition, all of the results presented in the following concern non-dimensional wake inflow obtained by division by the factor ΩR.

Dividing the blade span into a number of finite segments, the basis functions used in Eq. (2) are such to provide a linear distribution of inflow coefficients within each segment, assuring continuity at their edges.

3.1. Hovering condition

A coaxial counter rotating rotor system is characterized by a time periodic aerodynamic operator even for hovering flight conditions, with periodicity related to the number of blades of each rotor: in the present case its fequency is equal to 6Ω.

The wake model extracted considers the transfer functions corresponding to $N_m = 1$ in Eq. (3 (the rest of higher harmonics contributions have been proven to be negligible), and four rdial basis functions (this remains true for the next forward flight analysis, as well) .

The good quality of the RMA of the transfer functions extracted from the BEM solver is demonstrated in Fig. 1, which presents the frequency behavior of λ_1^{00} vs θ_0^+ (with θ_0^+ denoting the average of upper and lower collective pitches). A similar level of accuracy is observed

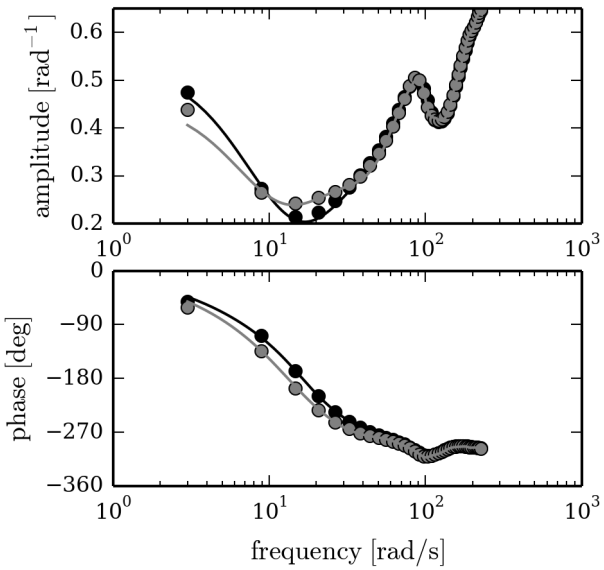

Figure 1: Transfer function λ_1^{00} vs θ_0^+ in hover. —— upper rotor RMA; —— lower rotor RMA; • sample upper rotor; • sample lower rotor.

for all of the transfer functions involved in matrix $\mathbf{H}$ for the hovering case.

Next, considering the following time history of θ_0^+ perturbation

$$\theta_0^+(t) = A\cos(\omega t)\sin(3\omega t)e^{-0.25t}, \quad (7)$$

with $A = 0.5$ rad and $\omega = 0.1\Omega$, the corresponding wake inflow perturbations predicted by the proposed methodology are correlated both with those directly computed by the BEM solver and with simulations of the inflow model in Ref.,[10] based on the Pitt-Peters-like linear approximation form (linear PP). This comparison is shown in Figs. 2 and 3 for the wake inflow evaluated at three blade sections, $r/R = \{0.4, 0.6, 0.95\}$, respectively on upper and lower rotor. These figures reveal that the Pitt-Peters-like model leads to a rough approximation of the inflow velocity, especially at the tip and at the root of the blades, whereas the proposed model provides very good predictions of the inflow at any spanwise position. The very good quality of the present model simulation is confirmed in Fig. 4 which shows the comparison with BEM predictions in terms of the frequency spectrum of the upper rotor inflow at $r/R = 0.6$. In particular, it is interesting to note that, although of small amplitude, also the contributions deriving from the 6/rev periodicity of the aerodynamic operator are very well captured by the proposed methodology.

An overview of the relevant enhancements introduced

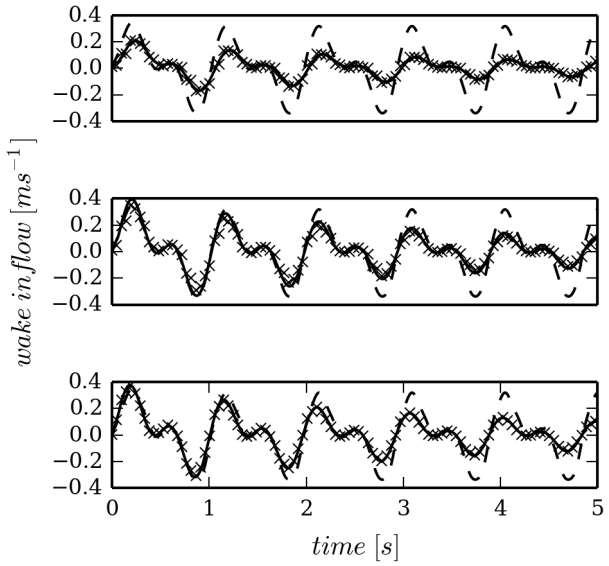

Figure 2: Wake inflow predictions on upper rotor at $r/R = 0.4$ (top), $r/R = 0.6$, $r/R = 0.95$ (bottom). Hover condition. —— present model; - - - Pitt-Peters-like model; xx BEM.

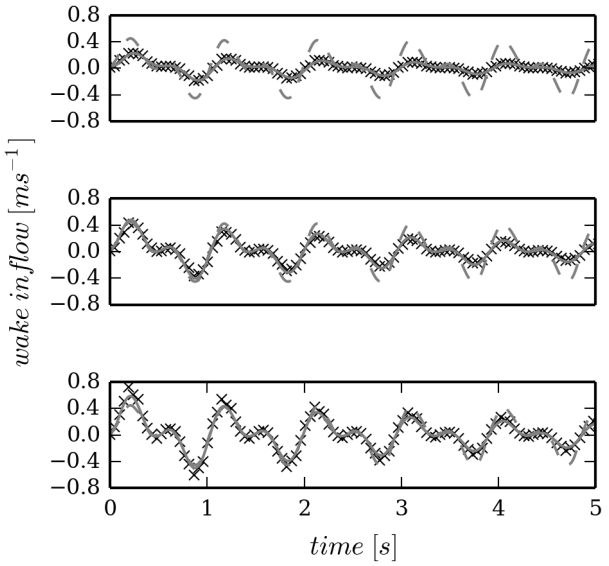

Figure 3: Wake inflow predictions on lower rotor at $r/R = 0.4$ (top), $r/R = 0.6$, $r/R = 0.95$ (bottom). Hover condition. —— present model; - - - Pitt-Peters-like model; xx BEM.

by the radial approximation proposed in this work is given in Fig. 5. It presents the spanwise distributions of the percentage of the error rms related to the sectional inflow peak, obtained by the present formulation and by the linear Pitt-Peters-like model.[10] The improvement of the inflow prediction provided by the present radial description is considerable throughout the blade span. Note that the vertical solid lines identify the blade sections examined in Figs. 2 and 3.

3.2. Forward Flight

In forward flight condition the aerodynamic operator is affected by 3Ω periodicity. Thus, the inflow model is extracted by considering a multi-harmonic description with $N_m = 2$ in Eq. (3).

First, considering a θ_0^- perturbation input equal to that employed for the hovering case for θ_0^+ (see Eq. (7)), Figs. 6 and 7 show the comparison between the wake inflow predicted by the present finite-state model and that directly provided by the BEM solver on the three blade sections examined above for the hovering condition. The two simulations are in quite good agreement, thus proving the capability of the introduced space-time-accurate finite-state model to describe with a good level of accuracy the wake inflow field over coaxial rotor systems.

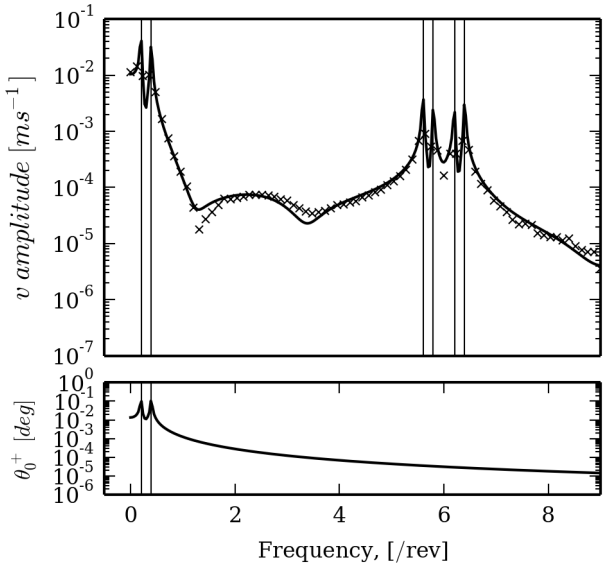

Figure 4: Induced velocity at $r/R = 0.4$ on the upper rotor. —— present model; xx BEM.

It is interesting to note that, contrarily to what is observed in hovering condition, in forward flight the time periodicity of the aerodynamic operator heavily affects the output. This is particularly highlighted in Fig. 8 which presents the frequency spectrum of the upper rotor inflow parameter λ_3^s: indeed, in this case, the am-

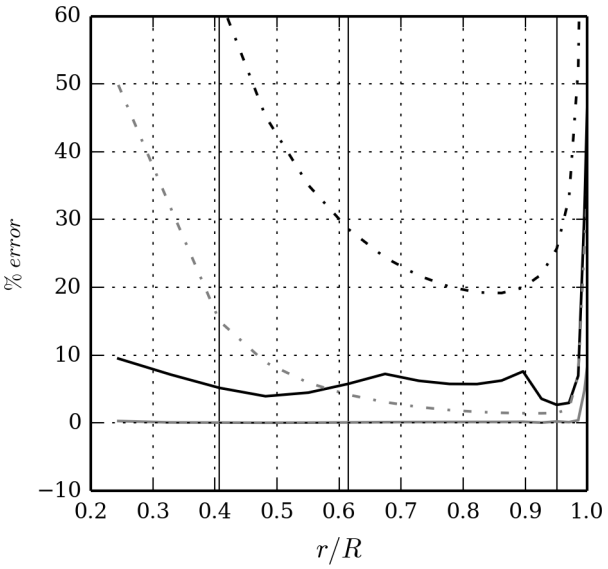

Figure 5: Spanwise error distribution for hovering condition. —— upper rotor present model; —— lower rotor present model; - - - - upper rotor Pitt-Peres-like model; - · - · - lower rotor Pitt-Peres-like model.

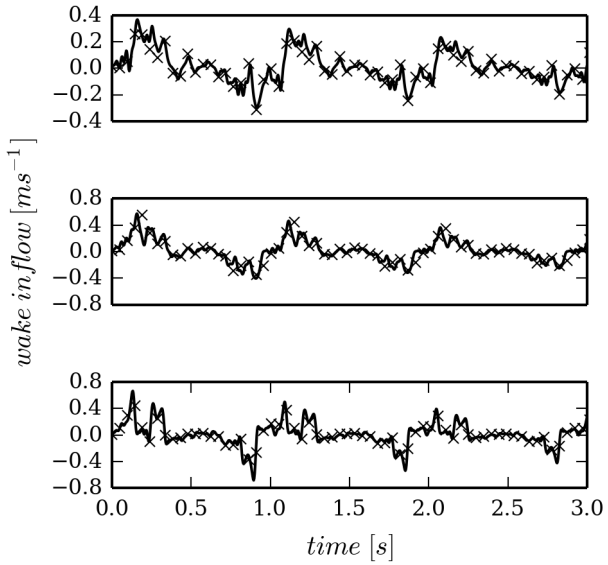

Figure 6: Wake inflow predictions on upper rotor at $r/R = 0.4$ (top), $r/R = 0.6$, $r/R = 0.95$ (bottom). Forward flight condition. —— present model; xx BEM.

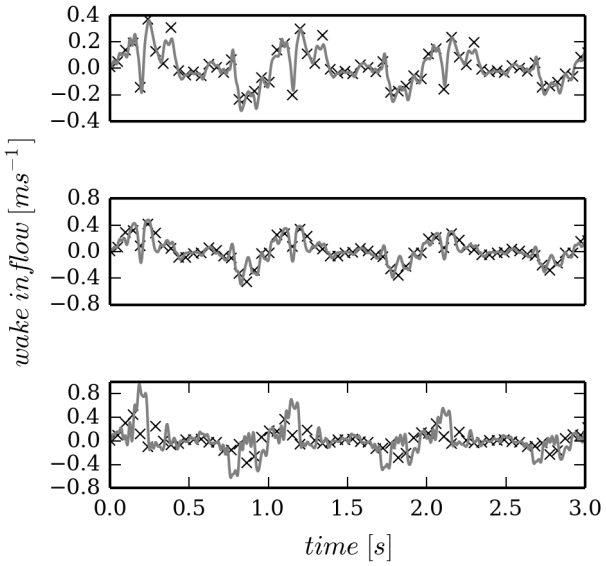

Figure 7: Wake inflow predictions on lower rotor at $r/R = 0.4$ (top), $r/R = 0.6$, $r/R = 0.95$ (bottom). Forward flight condition. —— present model; xx BEM.

plitude of the first multi-harmonic, 3/rev component is of the the same order of magnitude of the LTI component (namely, that at the same frequency of the input).

Finally, considering the spanwise distribution of the percentage prediction error shown in Fig. 9 (determined simarly to that of Fig. 5), it can be observed that, with respect to the linear Pitt-Peters-like model of Ref.,[10] introducing only a more detailed radial description and excluding multi-harmonics contributions leads to limited improvements of the overall quality of the inflow approximation. This confirms that for forward lfight conditions, combined time-space accurate descriptions are required for high quality inflow modelling.

4. CONCLUSIONS

From the numerical assessment of the proposed methodology for extraction of space-time accurate, finite-state, coaxial-rotor wake inflow models from high-fidelity aerodynamic solvers, the following conclusion are drawn:

- the radial variation of the wake inflow is captured with good accuracy by introduction of four basis functions per inflow coefficient, both for hovering and forward flight conditions;
- in coaxial rotor hovering conditions, (6/rev, for the case examined) multi-harmonic terms appear, but

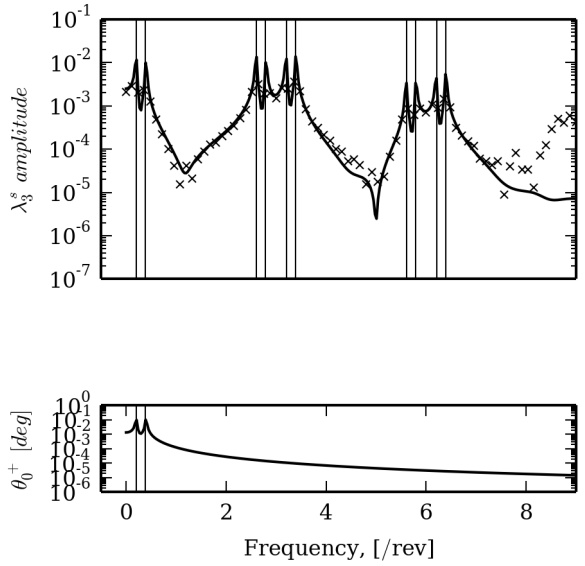

Figure 8: Upper rotor inflow parameter λ_3^s. —— present model; xx BEM.

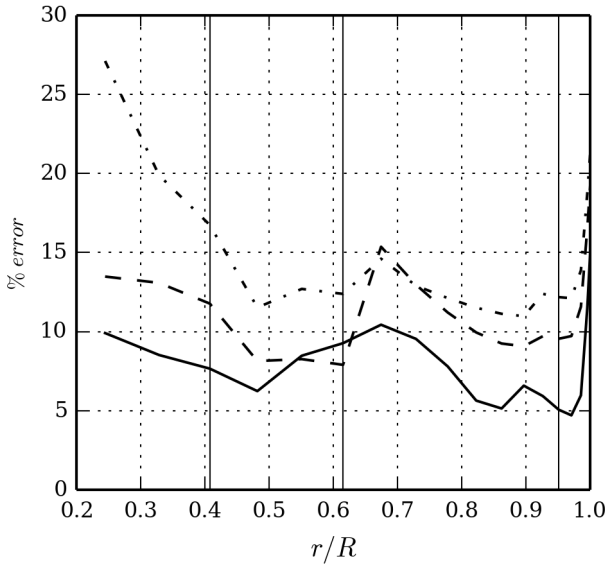

Figure 9: Spanwise error distribution for forward flight condition. —— upper rotor present model; - - - upper rotor w/o multi-harmonic termsl; - · - · - upper rotor Pitt-Peres-like model.

scarcely affects the quality of the inflow simulation;

- in forward flight conditions, (3/rev and multiples, for the case examined) multi-harmonic terms appear and may play a relevant role;

The preliminary results presented demonstrate the capability of the proposed finite-state modelling to capture multi-harmonic inflow terms deriving from the time-periodic nature of the coaxial rotor aerodynamic operator, and hence to predict with good space and time accuracy the wake inflow on advancing and hovering rotors. It seems to be an inflow simulation tool suitable for coaxial rotor aeroelastic stability and control applications.

COPYRIGHT STATEMENT

REFERENCES

[1] S. J. Newman, “The compound helicopter configuration and the helicopter speed trap,” *Aircraft Engineering and Aerospace Technology: An International Journal*, vol. 69, no. 5, pp. 407–413, 1997.

[2] A. J. Ruddell et al., “Advancing Blade Concept (ABC) Technology Demonstrator,” *Tech. Rep. USAAVRADCOM-TR-81-D-5, Sikorsky Aircraft Division of United Technologies Corporation*, 1981.

[3] C. P. Coleman *et al.*, *A survey of theoretical and experimental coaxial rotor aerodynamic research*, vol. 3675. National Aeronautics and Space Administration, Ames Research Center, 1997.

[4] J. G. Leishman, *Principles of helicopter aerodynamics*. Cambridge aerospace series, Cambridge, New York: Cambridge University Press, 2000.

[5] P. P. Friedmann, “Rotary-Wing Aeroelasticity: Current Status and Future Trends,” *AIAA Journal*, vol. 42, no. 10, pp. 1953–1972, 2004.

[6] D. M. Pitt and D. A. Peters, “Theoretical Predictions of Dynamic Inflow Derivatives,” *Vertica*, vol. 5, pp. 21–34, 1981.

[7] D. A. Peters and C. J. He, "Correlation of measured induced velocities with a finite-state wake model," *Journal of the American Helicopter Society*, vol. 36, no. 3, pp. 59–70, 1991.

[8] M. Gennaretti and G. Bernardini, "Novel boundary integral formulation for blade-vortex interaction aerodynamics of helicopter rotors," *AIAA Journal*, vol. 45, no. 6, pp. 1169–1176, 2007.

[9] M. Gennaretti, R. Gori, F. Cardito, J. Serafini, and G. Bernardini, "A space-time accurate finite-state inflow model for aeroelastic applications," in *72nd Annual Forum of the American Helicopter Society, West Palm Beach, Florida*, 2016.

[10] M. Gennaretti, R. Gori, J. Serafini, G. Bernardini, and F. Cardito, "Rotor Dynamic Wake Inflow Finite-State Modelling," *33rd AIAA Applied Aerodynamics Conference*, Dallas, TX, June 2015.

[11] F. Cardito, R. Gori, G. Bernardini, J. Serafini, and M. Gennaretti, "Finite-state dynamic wake inflow modelling for coaxial rotors," in 41^{st} *European Rotorcraft Forum*, (Munich, D), September 2015.

[12] D. M. Pitt and D. A. Peters, "Rotor dynamic inflow derivatives and time constants from various inflow models," in *15th European Rotorcraft Forum: September 13-15, 1983, Stresa, Italy*, 1983.

[13] R. Gori, F. Pausilli, M. D. Pavel, and G. M, "State-space rotor aeroelastic modeling for real-time helicopter flight simulation," *Advanced Material Research*, vol. 1016, pp. 451–459, 2014.